ISO observations of Pre-Stellar Cores and Young Stellar Objects *

Brunella Nisini
INAF Osservatorio Astronomico di Roma, Via di Frascati 33, 00040, Monteporzio Catone, Italy

Anlaug Amanda Kaas
Nordic Optical Telescope, Apdo 474, 38700 Santa Cruz de La Palma, Spain

Ewine F. van Dishoeck
Leiden Observatory, P.O. Box 9513, 2300 RA Leiden, The Netherlands

Derek Ward-Thompson
Department of Physics & Astronomy, Cardiff University, PO Box 913, Cardiff CF24 3YB, UK

Abstract. We summarize the observations of the Infrared Space Observatory concerning the earliest stages of the stellar formation. The observations of samples of sources in different evolutionary stages are reviewed, addressing in particular how the physical and chemical properties of the protostellar environments change from the pre-stellar cores to the protostars at the end of their accretion phase. In addition, the mid-IR surveys in nearby star forming regions are discussed showing their implications for the understanding of the stellar initial mass function.

Keywords: Star Formation, Young Stellar Objects, Protostars, ISO, Infrared Observations

Received: 9 July 2004

1. Introduction

The Infrared Space Observatory (ISO) (Kessler et al., 1996; Kessler et al., 2003) has represented a fundamental step in enlarging the observational data-set needed to understand the still poorly known earliest stages of formation of a new star.

Indeed, the spectral range covered by ISO (from 2 to 200 μm) is the most suited, both to identify new cold and heavily extincted protostars and to probe the different processes characterizing the interaction between young stars and their parental cloud. In particular, observations at mid- and far- infrared wavelengths are able to probe the gas and dust

* Based on observations with ISO, an ESA project with instruments funded by ESA Member States (especially the PI countries: France, Germany, the Netherlands and the United Kingdom) and with the participation of ISAS and NASA.

cooling of young stellar objects (YSO's) close environments, which is in turn a function of the different heating mechanisms and of their time evolution.

The formation of an isolated low mass star begins with the collapse of a cold dense core (pre-stellar core) where no source of internal heating is present. As soon as a centrally condensed protostar develops, the main heating mechanisms of circumstellar gas and dust become shocks, either due to matter accretion onto the disk and the protostellar surface, or developing along the energetic outflows (Class 0 sources, ages $\sim 10^4$ – 10^5 yr). Finally, when the protostellar phase is ending and the star approaches its pre-main sequence track, the accretion/ejection mechanisms become less and less important up to the point where the stellar radiation field starts to represent the main source of heating (Class I/II,$\sim 10^5$ – 10^6 yr). The heating processes in high mass protostars may follow a different time evolution. Indeed, due to their much shorter evolutionary time-scales, high mass sources develop large radiation dominated regions while they are still accreting their mass, but the mechanisms at work are the same as in low mass stars.

ISO has gathered both photometric and spectroscopic observations of samples of sources with different mass over all these evolutionary stages. In addition, it has performed extended surveys in nearby molecular clouds allowing the detection and classification of the young stellar and sub-stellar population of embedded clusters. This, in turn, has allowed us to extend the initial mass function (IMF) well into the brown dwarfs regime.

In this article we will review the main results obtained by such observations. In particular, we will concentrate on the main mechanisms giving rise to the gas and dust cooling in pre-stellar cores and young embedded sources (Class 0/I), with particular emphasis on the identification of specific evolutionary trends to be used in the exploiting of present and future IR space missions. The observation of more evolved YSOs (pre-main sequence Class II sources) and their disks will be reviewed by Lorenzetti and Jourdain de Muizon in this volume.

2. Pre-stellar cores

The formation of YSOs is known to occur in dense cores within molecular clouds (e.g. Williams, Blitz & McKee 2000). Study of such regions has been hampered in the past by their very large optical depths at near-infrared and optical wavelengths. It is only since the opening up of the far-infrared to submillimetre regime that astronomers have been

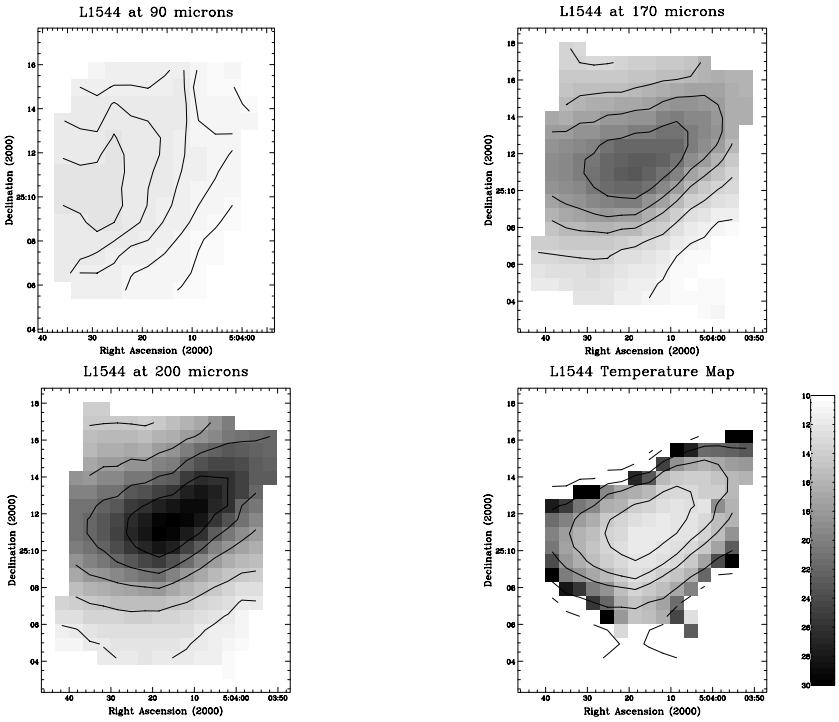

Figure 1. Grey-scale flux density images, with isophotal contour maps superposed, of the prestellar core L1544.

able to study molecular clouds in detail. ISO has played a key role in the progress that has been made.

Theories of star formation have, until recently, lacked a detailed observational determination of the initial conditions of the protostellar collapse phase (e.g. see: André et al. 2000 for a review). The pre-protostellar (or prestellar for short) core phase (Ward-Thompson et al. 1994) is the stage of star formation that precedes the formation of a protostar and hence should represent observationally the initial conditions of protostellar collapse.

Some recent observations have indicated that the Initial Mass Function (IMF) of stars may be determined at the prestellar core stage (Motte et al. 1998; Motte et al. 2001). Furthermore, theory predicts that the core geometry prior to this stage is critical in determining the manner of protostellar collapse (e.g. Whitworth & Summers 1985; Foster & Chevalier 1993; Whitworth et al. 1996). Therefore it is of vital importance to star formation theories to determine observationally the physical parameters of prestellar cores.

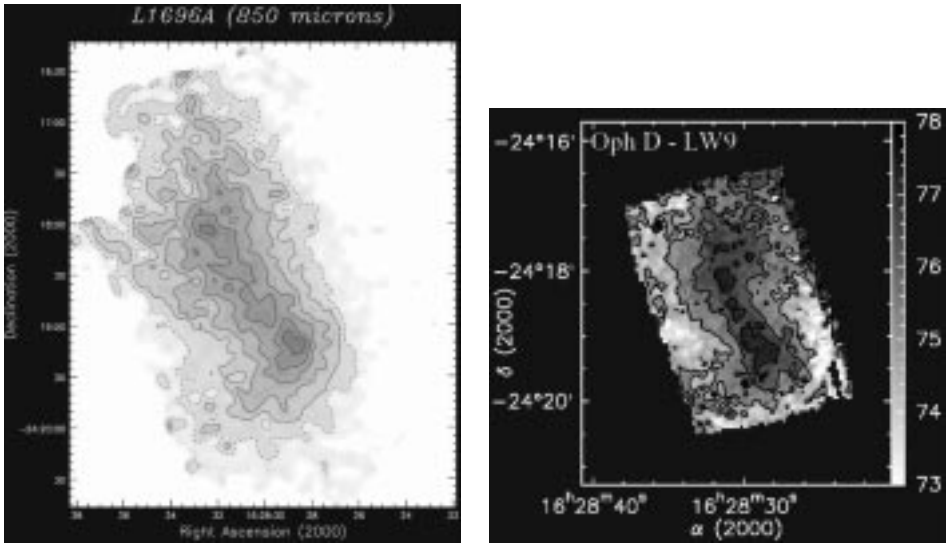

Figure 2. The prestellar core L1696A (also known as Oph D) seen in submm emission (left) and near-ir absorption (right). The similarity of the two maps shows that it is the same dust that is absorbing in the near-ir and re-emitting in the submm (images from Kirk et al. 2004 and Bacmann et al. 2000 respectively).

Molecular line surveys of dense cores by Myers and co-workers identified a significant number of isolated cores (Myers & Benson 1983; Myers et al. 1988; Benson & Myers 1989). Comparisons of these surveys with the IRAS point source catalogue identified those that already harboured embedded protostars, allowing those without them to be classified as starless cores (Beichman et al. 1986). Subsequent millimetre and submillimetre surveys allowed those starless cores that were most centrally condensed – the prestellar cores – to be identified (Ward-Thompson et al. 1994; André et al. 1996; Ward-Thompson et al. 1999).

The millimetre and submillimetre work showed that the cores all follow a form of density profile that is relatively flat in the centre and steeper towards the edge (Ward-Thompson et al. 1994). This is similar to the profiles predicted by theory to produce a decreasing accretion rate with time (Whitworth & Summers 1985; Foster & Chevalier 1993). The profiles are not consistent with the scale-free power-law profile predicted by the singular isothermal sphere (Shu 1977).

ISO was used to image a number of prestellar cores (Ward-Thompson et al. 2002), using the long-wavelength photopolarimeter ISOPHOT (Lemke et al., 1996; Laureijs et al., 2003). Figure 1 shows images of the pre-stellar core L1544 at each of three far-infrared wavelengths – 90, 170 and 200 μm. It can be seen that the core is very much less clearly

defined at 90 μm than at the other two wavelengths. This is due to the temperature of the core being very low. Typically prestellar cores have temperatures around 10 K (Ward-Thompson et al. 2002).

The colour temperature variation can be calculated across each core by first subtracting the background level and then ratio-ing the background-subtracted images at 170 and 200 μm. This can be converted to a colour temperature using the assumption of optically thin, modified black-body emission, namely:

$$(F_{\nu_1}/F_{\nu_2}) = \frac{\nu_1^{3+\beta}(e^{[h\nu_2/kT]}-1)}{\nu_2^{3+\beta}(e^{[h\nu_1/kT]}-1)},$$

where the frequencies ν_1 and ν_2 correspond to wavelengths of 200 and 170 μm respectively, and F_{ν_1} and F_{ν_2} are the flux densities at each of these frequencies. T is the dust temperature, β is the dust emissivity index (set to 2), and h and k are the Planck and Boltzmann constants respectively. Using these assumptions the colour temperature map in Figure 1 was made. Examination of this map shows that there is a temperature gradient approximately centred on the core, with the edge warmer than the centre. This is consistent with external heating by the local inter-stellar radiation field (ISRF).

ISOCAM (Cesarsky et al., 1996; Blommaert et al., 2003) was also used to observe prestellar cores. However, the cores are so dense that they do not emit at near- and mid-infrared wavelengths. Instead the cores are seen in absorption by ISOCAM (Bacmann et al. 2000) against the general background emission of the mid-ir interstellar radiation field at a wavelength of 7 μm.

Figure 2 shows the prestellar core L1696A (also known as Oph D) as seen in emission by SCUBA at 850 μm and in absorption at 7 μm by ISOCAM. The two maps show a very similar morphology. This indicates that the same dust that is absorbing in the near-ir is re-emitting in the submm. Calculations of the amount of the absorbed energy and emitted energy show they are roughly equal, implying that prestellar cores are in approximate energy equilibrium with their surroundings and have no embedded energy sources (Ward-Thompson et al 2002).

The fact that the same dust is being traced at 7 μm allows one to probe the structure of a prestellar core at the higher angular resolution of ISOCAM – 6 arcsec. This type of study showed that in fact prestellar cores are very sharp-edged. They can be modelled with profiles that reach density gradients steeper than $\rho \propto r^{-3}$ (Bacmann et al. 2000). These results are in direct contrast with singular isothermal sphere models. However, some magnetically regulated models may be able to reproduce the observations.

3. Low mass YSOs

Systematic studies of solar mass embedded YSOs have become possible only after the IRAS survey, which has provided the discovery and census of large samples of protostellar candidates. The combination of ground based and IRAS observations is still one of the main tools to define the relative evolutionary state of different YSOs, based on the steepness of their spectral energy distribution (SED) from near to far-IR (e.g. Lada 1999, André et al. 2000).

ISO has provided two fundamental improvements with respect to the information given by IRAS. Firstly, it has given the possibility to extend the observations of protostellar SEDs up to 200μm, which is where the youngest protostars (i.e. the Class 0 sources) have their emission peaks. Secondly, it has given for the first time, through its spectroscopic capabilities, the tools to probe the physical and chemical conditions of the warm circumstellar gas in large samples of sources, and to study their temporal evolution. These two aspects will be separately discussed in the following sections. Recent reviews on ISO observations of low mass YSOs, which address these and other aspects of the subject can be found in van Dishoeck (2004), Nisini (2003), Saraceno et al. (1999).

3.1. Spectral energy distribution (SED)

The shape of the YSOs SEDs in the mid- and far-infrared is a sensitive function of the temperature and density structure of their circumstellar envelopes and of the geometry of the dust distribution. Such a shape has been reconstructed with unprecedented details through both the photometric data by CAM and PHOT, and the spectro-photometric observations provided by SWS (de Graauw et al., 1996; Leech et al., 2003) and LWS (Clegg et al., 1996; Gry et al., 2003) .

Most of the analysis has been focussed on the young Class 0 protostars, which have their bulk of emission in the FIR and sub-mm range. Adopting a simple model of greybody emission from a spherical envelope, Froebrich et al. (2003) derived the L_{bol} and T_{bol} of seven young protostars using ISOPHOT data in conjunction with other sub-mm observations. The typical temperatures found range between 20 and 35 K. The location in a L_{bol}-T_{bol} diagram, compared with evolutionary tracks for young protostars, have been in turn used to infer their ages, which span from 15000 to 30000 yr, thus confirming the youthness of the objects. The SEDs of many IR/SMM sources in the Serpens cloud have been extracted from an LWS raster map of the region by Larsson et al. (2000). They show that most of the observed SEDs can be well represented as modified single-temperature blackbodies, as previously

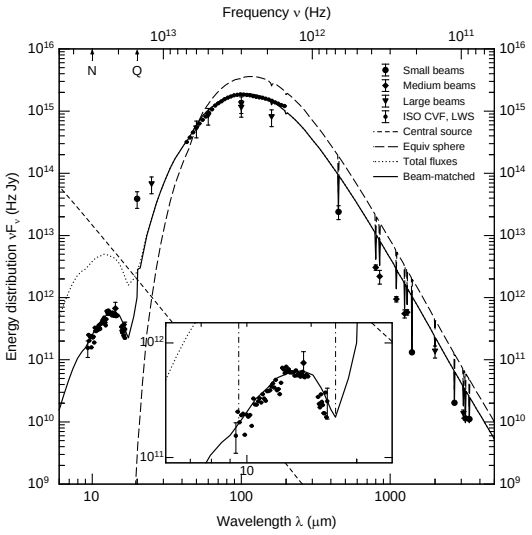

Figure 3. SED of the Class 0 source SMM1/FIRS1 from 10μm to 3mm, with superimposed a model fit assuming an envelope emission where two bipolar cavities are escavated by the source outflow (solid line). The SED for the equivalent spherical envelope is also shown. From Larsson et al. 2002.

assumed, but that the derived temperatures are generally higher than what has been found by means of IRAS observations, which also implies higher L_{bol} values. For the individual Class 0 source SMM1/FIRS1 the model for an envelope with two escavated regions of lower densities produces a better fit also to the mid-IR ISOCAM data of the source (Larsson et al. 2002, Figure 3).

Other young protostars studied with a similar analysis includes IRAS16293-2422 in ρ Oph (Correia et al. 2004), and several sources of the Cederblad 110 nebula in the Cham I molecular cloud (Lehtinen et al. 2001).

The SEDs of the more evolved Class I sources do appear much broader than those of the Class 0 sources, due to their more tenuous envelopes which allow to see their inner and warmer regions mainly emitting in the mid-IR. A detailed account for the SEDs from the near to the sub-mm have been given for two of these sources, namely L1551-IRS5 (White et al. 2000) and Elias 29 (Boogert et al. 2002).

In both cases, and at variance with the Class 0 SEDs, good fits to the observed data require the inclusion of different emission components taking into account the presence of both a flaring disk and a more extended envelope. In Elias 29, in particular, a large and massive (up to 0.012 $M_\odot$) disk has been suggested to explain the observed SED flattness between 10 and 200μm (Figure 4).

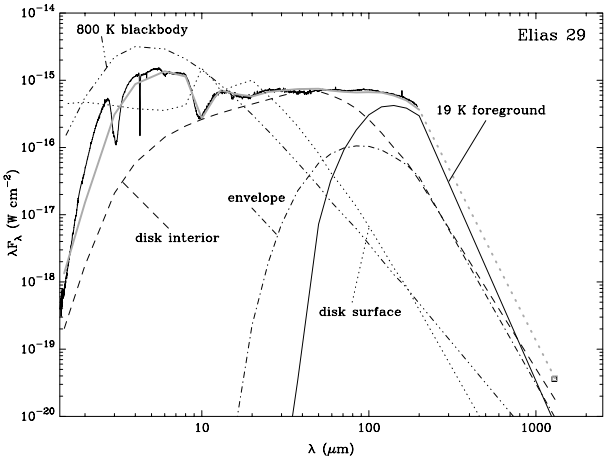

Figure 4. SED of the Class I source Elias 29 as observed by ISO SWS and LWS, combined with ground-based 1.3mm flux (Boogert et al. 2002). The SED has been fitted by a model considering four different components, namely a blackbody emission from the inner envelope, a flaring disk, an outer envelope and a foreground cloud.

3.2. Gas cooling and spectral evolution of protostars

ISO has gathered SWS, LWS and CAM-CVF spectra of samples of low mass YSOs with different luminosities and evolutionary stages, providing a fundamental and unique data-base to probe the gas physical conditions and their time evolution in the protostellar envelopes.

The SWS and CAM-CVF spectra of low luminosity sources usually present only broad features due to abundant ices seen in absorption against the young source. These originates in the outer envelopes, consequently they are more sensitive to the amount of foreground dust and its chemical composition than to the conditions close to the source (Boogert et al. 2002, Alexander et al. 2003).

The LWS spectra, on the other hand, are rich of lines in emission whose excitation mechanisms can be directly reconducted to intrinsic properties of the source itself, allowing us to discriminate among the different excitation mechanisms which dominate the gas heating of circumstellar envelopes during the protostellar evolution.

LWS spectral surveys of samples of low luminosity Class 0 and Class I sources have been discussed in Giannini et al. (2001) and Nisini et al. (2002), while the spectra of individual objects have been analyzed by different authors (see van Dishoeck 2004 for a complete list of references).

The far-IR spectra of embedded YSOs indicate low excitation conditions in their envelopes, since only emission from the atomic lines

[OI]63 and 145μm and the single ionized line [CII]158μm, as well as from molecular transitions of abundant species (CO, H_2O, OH), are detected. Such lines probe gas temperatures and densities in the range $\sim$100–2000 K and 10^4–10^7 cm^{-3}, respectively.

The main observational evidence which appears from the analysis of the spectra of different sources, is that while the spectra from the Class 0 are dominated by both atomic and molecular emission, very few molecular lines, and only in form of CO and sporadically OH, are detected in Class I sources. Quantitatively, the total gas cooling due to molecular emission with respect to the bolometric luminosity decreases by about an order of magnitude going from Class 0 to Class I sources (see Figure 5). In Class 0 objects, water has been detected in 13 out of 17 observed sources, and its abundance is much higher (10^{-4}–10^{-5}) than in quiescent clouds with a trend to increase with the kinetic temperature.

Several authors suggest that the main mechanism for gas excitation are the strong shocks expected to occur as the energetic protostellar jets impact towards the dense envelopes (see e.g. Giannini et al. 2001, Nisini et al. 2002, Larsson et al. 2002, Molinari et al. 2000, Froebrich et al. 2002). Different evidences are in favour of this interpretation: the physical conditions and relative abundances of the observed species, derived from the analysis of observed lines, are very similar to those inferred in shocked regions far from the source and can be explained in the framework of low velocity and dense shocks (see Sect. 5). In addition, the strongest molecular emission is observed towards sources where dense and warm molecular jets are present close to the object. Finally, there is a direct correlation between the total luminosity radiated by the traced gas component and the kinetic luminosity associated to the protostellar outflow. In the framework of shock excitation, the observed difference in the far IR spectra of Class 0 and Class I objects can be explained by considering that the protostellar envelope with time becomes more diffuse and escavated. Thus, the protostellar jet encounters a smaller ambient density, which gives rise to preferentially dissociative shocks, causing a significant decrease of the contribution of the molecular luminosity to the total gas cooling (Nisini et al. 2002).

A different scenario is proposed by Ceccarelli et al. (2000) and Maret et al. (2002) which suggest that most of the water and [OI] emission observed in Class 0 sources is originated from the innermost regions of protostellar envelopes, where the relatively high dust temperatures can favour the evaporation of gaseous H_2O from the grain mantles. Such an hypothesis is supported by a detailed model of the envelope thermal structure and radiative transfer which provide a good fit of the observed water line emission in NGC1333-IRAS4 and IRAS16293-2422,

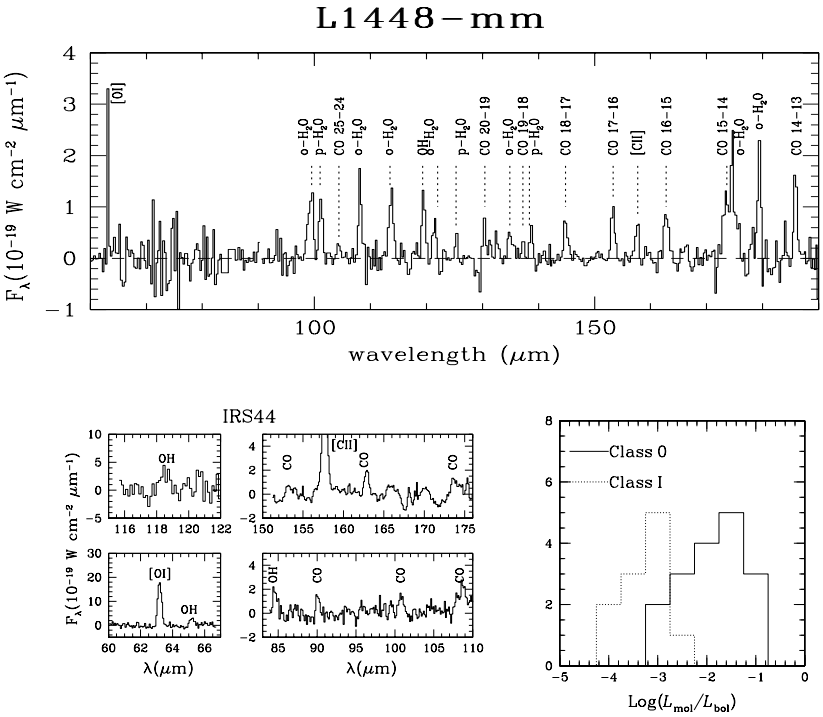

Figure 5. Continuum subtracted ISO-LWS spectrum towards the Class 0 source L1448-mm (upper) and the Class I source IRS 44 (bottom left). While the Class 0 source spectrum is very rich of molecular emission, especially H_2O, the Class I spectrum has only few weak lines from CO and OH. (Bottom right) Histograms of the cooling due to molecular emission with respect to the bolometric luminosity for the Class 0 and Class I systems observed by ISO-LWS (Nisini et al. 1999, 2002).

with mass accretion rates of few times 10^{-5} $M_\odot$ yr. In this framework, the decline of water emission in Class I sources is explained by the water dissociation as soon as the source developes a significant FUV field. This hypothesis however requires a different mechanism to explain the strong CO emission always associated with the H_2O lines, which cannot be reproduced in the envelope model. Ceccarelli et al. (2002) suggest that such CO emission in the Class I source Elias 29 could be originated in the circumstellar disk, an hypothesis which seems however difficult to explain the high CO temperatures (T=300-1500 K) derived in most of the Class 0 sources.

4. High-mass YSOs/UC HII regions

In contrast with the case of low-mass YSOs, there is no well-established scenario for the evolution of high-mass YSOs. Many different observational phenomena are known to be associated with high-mass star formation — including radio emission from UltraCompact (UC) HII regions, H_2O and CH_3OH maser emission, millimeter lines of complex organic 'hot core' molecules, and bright mid-infrared continuum—, but these have not yet been put in a clear evolutionary sequence. Moreover, most high-mass stars form in groups with the various YSOs often at slightly different evolutionary stages. For example, hot cores are often found within a few arcsec of UC HII regions (see Kurtz et al. 2000, Churchwell 2002 for reviews). Within the ISO beams, these objects are usually blurred together, although often a single object dominates the mid- and far-infrared fluxes.

A prototype example of a high-mass star-forming region is provided by Orion BN-KL. Within the large ISO beams, the Becklin-Neugebauer object dominates the flux at shorter wavelengths (<10 μm), whereas IRc2 is stronger at longer wavelengths. Due to the interaction of the massive young stars with their surroundings, a wealth of spectral features is revealed beautifully in SWS spectra by van Dishoeck et al. (1998), González-Alfonso et al. (1998, 2002), Wright et al. (2000) and Rosenthal et al. (2000), and in LWS data by Harwit et al. (1998) and Cernicharo et al. (1999). All phenomena associated with massive YSOs are reflected in the spectra, including foreground ionized gas, PDRs, shocks, and the warm gas associated with the deeply embedded YSOs themselves.

In spite of these limitations, ISO observations have clearly contributed to our understanding of the evolution of high-mass YSOs, both in the deeply embedded early stages and in the more evolved H II region phase. The bulk of the new results are due to low- to medium resolution spectroscopy with the SWS and LWS, which also provide a complete characterization of the SED.

4.1. Deeply embedded high-mass YSOs

The youngest high-mass pre-stellar cores and deeply embedded YSOs emit primarily at far-infrared wavelengths. The ISOPHOT Serendipity Survey has revealed a number of cold compact objects at 170 μm coinciding with sources detected at long wavelengths with other facilities (e.g., Krause et al. 2003). These objects have low average dust temperatures (12–16 K) and masses up to a few hundred $M_\odot$, and are thus excellent candidates for massive protostars.

About a dozen embedded high-mass YSOs have been observed with the SWS and LWS (e.g., Gerakines et al. 1999, Gibb et al. 2004). The combined SWS-LWS spectra show that the continuum flux peaks at 60–90 μm, characteristic of black-body emission of $\sim$30 K. Some sources are brighter at mid-infrared wavelengths around 12 μm, indicating the presence of warmer dust along the line of sight with temperatures up to a few hundred K.

The SWS spectra are characterized by deep amorphous silicate and ice bands, which can absorb more than 50% of the continuum flux in the 2–20 μm region. Very few other features are seen in these deeply embedded stages: no PAH emission is apparent, and there are virtually no gas-phase molecular lines. Only a few atomic lines are detected in the LWS spectra, mostly the [C II] and [O I] fine-structure lines associated with nebulosity or PDRs. Thus, these objects do not resemble Orion BN-KL, even when scaled for the larger distance.

In spite of their similar SEDs, the embedded objects do show evidence for progressive heating of the envelope. This is most clearly reflected in the shape of a number of ice absorption bands, most notably the 15 μm CO_2, 4.3 μm $^{13}CO_2$ and 6.8 μm unidentified features (Gerakines et al. 1999, Boogert et al. 2000, Keane et al. 2001). In addition, the gas/solid abundance ratio of species like CO and H_2O (e.g., Boonman & van Dishoeck 2003), and the excitation temperatures of gaseous C_2H_2 and HCN (Lahuis & van Dishoeck 2000) show a similar trend which correlates well with the far-infrared color as defined by the 45/100 μm flux ratio. Thus, the objects can be put in a temperature sequence. Since these diagnostics involve absorption in a pencil beam along the line of sight as well as emission from the entire envelope, the heating must be 'global'. The most likely scenario, put forward by van der Tak et al. (2000), is that the warmer sources have a lower ratio of envelope mass $M_{\rm env}$ compared with L_{bol}. If the lower $M_{\rm env}$ are due to gradual dispersion of the envelope rather than different initial conditions, the heating sequence would correspond to a time sequence. Thus, the mid-infrared spectral features provide a unique and powerful diagnostic of the first few $\times 10^4$ yr of protostellar evolution.

4.2. UC H II regions

When the envelope is dispersed and the H II region developed, the spectral characteristics of massive YSOs change dramatically. An excellent example is provided by the comparison of Cep A with S 106 (see Figure 6, van den Ancker et al. 2000). Both sources have luminosities of $2 - 4 \times 10^4$ $L_\odot$, but the spectrum of Cep A is characteristic of the deeply embedded sources discussed above, whereas the S 106 spectrum

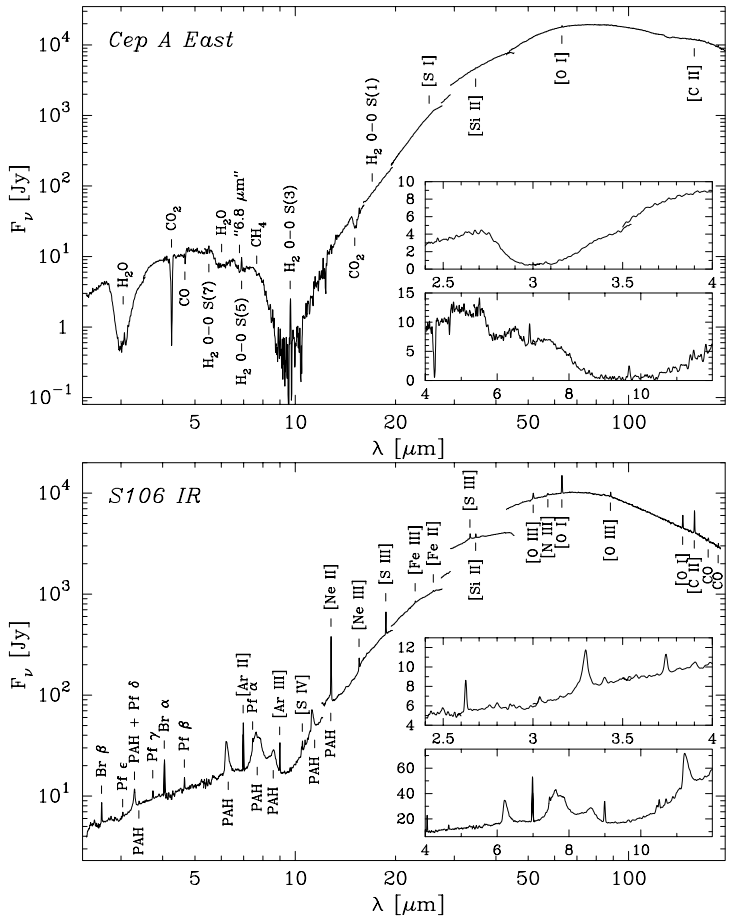

Figure 6. Combined SWS-LWS spectra of two massive YSOs at different evolutionary stages. Cep A ($2.4 \times 10^4 L_\odot$) is in the deeply embedded phase, whereas S 106 ($4.2 \times 10^4 L_\odot$) is in a more evolved stage where it has developed a compact H II region and a PDR (van den Ancker et al. 2000).

is dominated by PAHs and by atomic lines from a wide range of ionization stages characteristic of a young O8 star. The atomic and molecular H_2 and CO emission lines indicate that shock excitation dominates for Cep A, but PDR excitation for S 106.

Peeters et al. (2002) present combined SWS-LWS spectra for a sample of 45 compact H II regions, and Giveon et al. (2002) analyse SWS spectra of 112 galactic H II regions. The SEDs of the compact H II regions peak at 40–60 μm, corresponding to $T_d \approx 60 - 70$ K, clearly warmer than those of sources in the deeply embedded phase. The spectra are dominated by PAHs and ionized atomic lines. Since the sources cover a wide range of galactocentric radii ranging from 0 to 18 kpc, the

line ratios are used to study variations in the excitation, metallicity, and hardness of radiation field on a galactic scale. No attempts have yet been made to use these features to study evolutionary effects within the H II region sample.

At an even later stage, the young stars have completely broken free from their parental clouds and the young O and B stars emit copious ultraviolet photons, which can create PDRs at the edges of neighboring molecular clouds. Examples are given by M 17, Orion and Trumpler 14, with the latter source harboring a cluster of at least 13 O stars (Brooks et al. 2003). They are readily recognized by strong atomic fine-structure lines and H_2 emission, and have been reviewed in detail by Hollenbach & Tielens (1997) prior to ISO. New insights due to ISO are summarized by van Dishoeck (2004).

5. Outflows and HH objects

Shocks originated in outflows cools mainly radiatively through line emission in a wide range of wavelengths, from UV to the radio (Reipurth & Bally 2001). In particular, shocks occurring in dense environments cool down preferentially through emission lines in the mid and far IR, mainly through the [OI]63μm transition and the pure rotational transitions of H_2, CO and H_2O (see e.g. Hollenbach 1997).

Due to the limited spectral and spatial resolution of the ISO observations, they do not allow in most cases to resolve the emission regions along the jets; nevertheless, they give unique information on global properties of the warm shocked gas, such as the total radiative cooling in the post-shocked layers and the relative abundances of species which in turn can be used to give tight constraints on the physics of the shocked region.

Most of the well known molecular outflows from very young stars have been observed by ISO-LWS and SWS (see van Dishoeck 2004 for a complete references list of the observed shocked regions). The physical conditions derived from the molecular emission are consistent with moderately warm and dense gas (n=10^4-10^6 cm^{-3}, T=300-1500 K) emitted by compact regions. Indeed strong molecular emission is evidenced mainly in young outflows showing the presence of localized components of very high velocity gas (v>50 km s^{-1}). The far infrared gas cooling can be a significant fraction of the total shock cooling in outflows from young embedded protostars, often representing more than 90% of the total radiated power (e.g. Nisini et al. 2000). Such a shock radiated power is $\sim 10^{-2}\, L_{bol}$ in outflows from Class 0 sources,

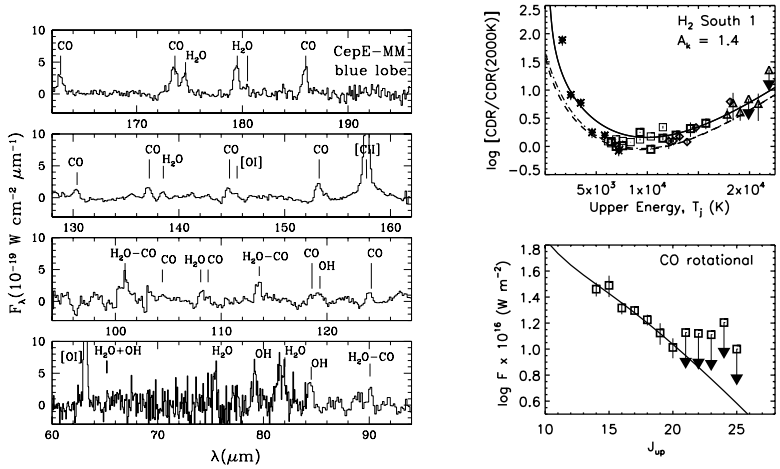

Figure 7. Left: LWS spectrum of the Cep E outflow (Giannini et al. 2001). Right: C-type bow shock model fit for Cep E, blue lobe, through ground-based roto-vibrational and ISO pure rotational H_2 lines (upper panel) and LWS rotational CO lines (bottom panel). From Smith et al. (2003).

while it is about an order of magnitude smaller for Class I outflows, indicating a clear decline of the outflow power with the evolution.

The presence, in most of the observed spectra, of both strong [OI]63μm emission and strong molecular emission in form of CO and H_2O supports the view where the interaction between the jet and the ambient medium occurs through a bow shock, where a high velocity shock, mainly emitting in atomic transitions, is produced at the bow apex, while the molecular emission comes from lower velocity shocks in the bow wings. Such a bow structure is also able to produce the stratification of temperatures needed to take into account the H_2 emission spectra, which show both low excitation pure rotational lines, as detected by SWS and CAM-CVF, and the roto-vibrational lines at higher excitation observed by ground (e.g. Wright et al. 1996, Moro-Martín et al. 2001, Wilgenbus et al. 2002, Rosenthal et al. 2000). Detailed models for bow shocks have been succesfully tested and applied to the ISO observations of several outflows (e.g. Froebrich et al. 2002, Smith et al. 2003, see Figure 7).

Giving their low excitation temperature, the H_2 0–0 lines can be also used to show deviations of the ortho-para ratio from the equilibrium value. In the Herbig-Haro object HH54, an ortho-para ratio ~ 1 has been estimated which implies that the gas has not yet reached the equilibrium and it is therefore very young (Neufeld et al. 1998, Wilgenbus et al. 2000).

In addition, the unique possibility offered by ISO to observe for the first time many transitions of thermally excited H_2O, has allowed to test predictions about the water formation in shocks and its importance in the gas cooling. Indeed, in magneto-hydrodynamic C-type shocks, water is expected to be one of the major coolant of the post-shocked gas, due to its rapid formation through chemical reactions which transform all the available neutral oxygen into H_2O as soon as the gas temperature increases above $\sim$ 400 K (e.g. Kaufman & Neufeld, 1996). Pure rotational lines of H_2O have been indeed observed in several outflows and high abundances (10^{-5}–10^{-4}) are often measured (Liseau et al. 1996, Harwit et al. 1998, Nisini et al. 2000, Giannini et al. 2001), which are much higher than the abundances measured in quiescent molecular clouds.

The ISO spectra of many optically visible HH objects, show the presence of line emission also from the fundamental levels of ions, such as [FeII], [SiII], [OIII], [NII] and [NeII] which trace the presence of high excitation dissociative shocks (e.g. Molinari et al. 2001, White et al. 2000, Lefloch et al. 2003). Electronic densities derived through ratios among these lines are higher by at least an order of magnitude with respect to those inferred in the optical. Finally, from the luminosity of the [OI]63μm line observed in a sample of HH object, Liseau et al. (1997) have determined the mass loss rates of the HH exciting sources, which result to be in good agreement with those extimated in the associated CO outflow, implying that the two phenomena are strictly connected.

6. YSOs census in nearby clouds

The origin of the stellar Initial Mass Function (IMF) is one of the most fundamental problems in astronomy. By studying statistically significant samples of YSOs in nearby clusters we hope to understand the relation between the final stellar IMF and the various phases of the star formation process. The observational challenge in obtaining a census of YSOs is 1) to detect the objects, as they are frequently embedded in dense clouds ($A_V \sim$ 10-100 mag) and 2) to distinguish cluster members from field stars.

The main objective of the ISOCAM surveys LNORDH.SURVEY_1 and GOLOFSSO.D_SURMC within the ISO central programme was to make a deep search of YSOs in selected parts of nearby star formation regions in order to sample objects down to $\sim$ 0.03 $L_\odot$. In terms of masses this corresponds to $\sim$ 0.05 $M_\odot$ for typical ages of $\sim 10^6$ yrs of T Tauri type stars (Class II objects). The two broad band filters

Table I. Overview of the surveyed regions.

Region	D(pc)	A(sq. deg.)	Ref.
NGC1333	300	0.19	
L1551	140	0.12	Gålfalk et al. 2004
L1527	140	0.26	
L1641	480	0.02	
NGC2023	480	0.43	see Abergel et al. 2002
LBS23	480	0.14	
NGC2071	480	0.28	
NGC2068	480	0.15	
Cha I	160	0.59	Nordh et al. 1996, Persi et al. 2000
Cha II	178	0.20	Nordh et al. 1996, Persi et al. 2003
Cha III	150	0.10	Nordh et al. 1996
ρ Oph L1688	140	0.56	Bontemps et al. 2001
ρ Oph L1689N	140	0.07	Bontemps et al. 2001
ρ Oph L1689S	140	0.07	Bontemps et al. 2001
Serpens Core	260	0.13	Kaas et al. 2004
Serpens NH3	260	0.09	Kaas et al. 1999
RCrA	130	0.45	Olofsson et al. 1999
Cep A	730	0.09	Gålfalk, 1999

LW2 (5-8.5 μm) and LW3 (12-18μm) had been designed to avoid the silicate features around 10 and 20 μm, and to trace well the mid-IR SED of YSOs. Before ISOCAM our knowledge of the stellar content in these regions was in most cases limited to observations in the optical, the near-IR, and from the IRAS survey. Ground-based mid-IR surveys were few and limited to the LMNQ bands (see e.g. Lada & Wilking, 1984, Greene et al. 1994).

6.1. Improved samples of IR-excess sources

The 10 times higher spatial resolution of ISOCAM (3-6"/pix) resolved much of the source confusion for clustered regions experienced with IRAS. The results of the photometry in the two broad bands LW2 (6.7 μm) and LW3 (14.3 μm) showed that the nominal integration times of 15-60 s gave a sensitivity of $\sim$ 2 mJy. In Fig. 8 (left) we have shown the [14.3/6.7] versus $F_\nu(14.3)$ diagram for several hundred sources in some of the star formation regions explored. A general result for all regions is the clear bimodal distribution in terms of colour - a blue (open triangles) and a red (filled circles) group. The blue colour is

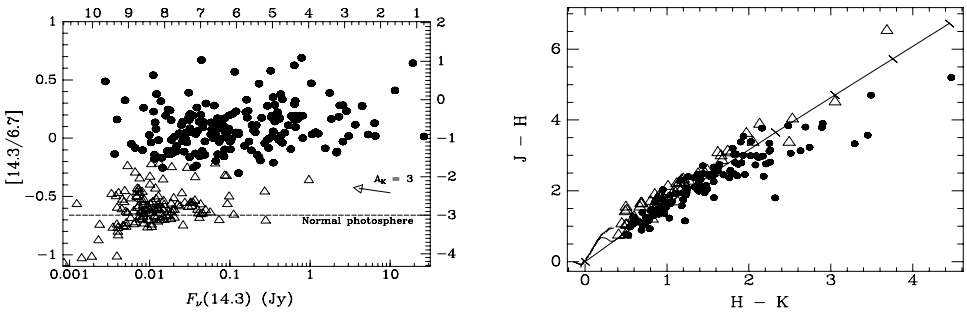

Figure 8. **Left:** The clear separation between IR-excess sources (filled circles) and sources without IR-excess (open triangles) is shown in the ISOCAM colour-magnitude diagram [14.3/6.7] versus $F_\nu(14.3)$. The colour index [14.3/6.7] is defined as the logarithm of the flux ratio, and as an alternative the SED index $\alpha = d\log(\lambda F_\lambda)/d\log\lambda$ calculated between 6.7 and 14.3 μm is shown on the right hand y-axis. The top x-axis indicates the 14.3 μm band magnitude. The effect of 30 mag of visual extinction is indicated with an arrow. **Right:** The same sources shown in the $J-H/H-K$ diagram. From Kaas & Bontemps (2000).

as expected for normal photospheres, i.e. the slope in the Rayleigh-Jeans tail. This group thus contains a mixture of field stars and cluster members without IR excesses. The red sources have colours typical of classical T Tauri stars (CTTS) with mid-IR excesses arising from optically thick circumstellar disk emission.

Comparing the same sources in the near-IR $J-H/H-K$ diagram demonstrates a merging of these two groups around the reddening line (Fig. 8 right). On average only 50% of the IR-excess population found with ISOCAM can be extracted by using the $J-H/H-K$ diagram. Thus, the ISOCAM surveys have revealed IR-excess populations about twice as large as previously known, thereby providing the to date most complete samples of the youngest YSOs. In RCrA only 1/3 of the ISOCAM selected IR-excess sources were previously known YSOs, and in L1551 only 12%. Note that while most ISOCAM sources are *detected* in deep near-IR surveys, it is the clear separation of IR-excess from cloud reddening which is the strength of the mid-IR.

YSOs without IR-excesses can not be distinguished from field stars by the use of broad band photometry alone. Therefore, the ISOCAM surveys do not sample these sources and can not be used to directly evaluate the number fraction of disks among YSOs. Other search tools such as e.g. X-ray surveys, optical spectroscopy or proper motion studies must be applied to make a census of this part of the YSO population. Only approximate estimates of disk fractions based on previous studies and galactic models of the mid-IR point source sky can be given, and

these estimates give disk fractions from 65 to 100%, the largest value being for the central Serpens Cloud Core (see below).

6.2. Nature and spatial distribution of IR-excess sources

As emphasized by Nordh et al. (1996) the [14.3/6.7] colour for the IR-excess sources is essentially constant - although with a spread - over a 14.3 μm flux interval of almost 4 orders of magnitude, showing that the source characteristics are similar over a very wide range of luminosities. Also, the different types of IR excess YSOs: Class I and Class II sources, and the so-called flat-spectrum sources in a transition phase between them, were found to have about the same mid-IR colour on average (see also Alexander et al. 2003). To classify the IR-excess YSOs we used the SED index $\alpha = d\log(\lambda F_\lambda)/d\log\lambda$ calculated between 2.2 and 14.3 μm. While the Class I/Class II number ratio is 5/42 for Cha I and 16/123 for ρ Oph, as expected based on current ideas about the time scales for each evolutionary class, this ratio is 19/18 for the central Serpens Cloud Core. Together with the very strong sub-clustering of the Class I and flat-spectrum sources (0.12 pc diameter) this suggests a very recent burst of star formation in Serpens. The Class II sources also show sub-clustering, but on scales of 0.25 pc and with an additional scattered distribution, similar to what was found in ρ Oph. In Cha I there is also sign of sub-clustering of Class II sources, but the clusters being slightly more extended, about 0.5 - 0.7 pc.

6.3. The Initial Mass Function (IMF)

The improved Class II samples provide luminosity functions (LFs) with completeness limits at about 0.07 $L_\odot$ for RCrA, 0.06 $L_\odot$ for Cha I, 0.03 $L_\odot$ for ρ Ophiuchi, and 0.08 $L_\odot$ for the Serpens Core. The LFs reach down to below 0.01 $L_\odot$, however, and it turns out that 20% of the Class II sources in Cha I, ρ Ophiuchi and Serpens are putative young brown dwarfs with disks. In RCrA about 30% of the ISOCAM selected YSOs are substellar candidates.

As shown in Fig. 9 a) the 123 Class II sources in ρ Ophiuchi produce a rather flat LF below ~ 2 $L_\odot$. Furthermore, as shown by Bontemps et al. (2001) each of the four sub-clusters A, B, EF, and L1689S have individual LFs of this same shape. The Class II LF can be modeled with an IMF flat below 0.55 $M_\odot$ (see Fig. 9 b) down to 0.06 $M_\odot$. There is no evidence for a turnover of the mass function at low masses. The Class II mass function is indistinguishable from the mass spectrum of the pre-stellar condensations (Motte et al. 1998), which suggests that the origin of the IMF is found at the early fragmentation stage of star formation.

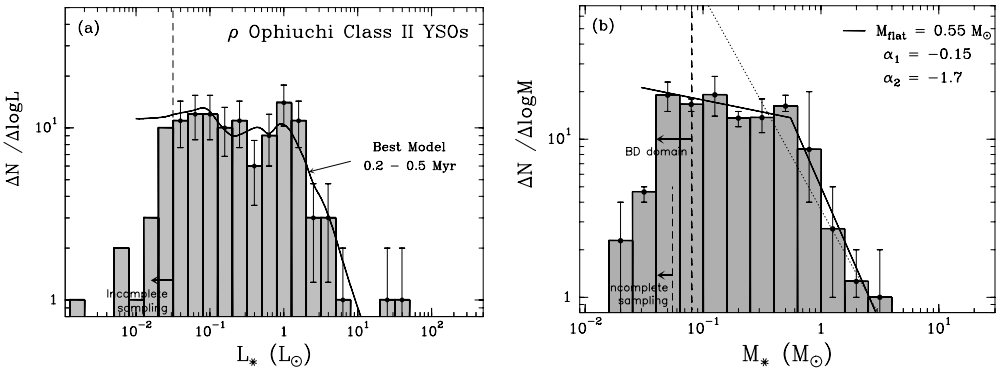

Figure 9. **a)** The Class II LF for ρ Ophiuchi. Dashed vertical line shows the completeness limit. Bold curve shows the best model LF, which is obtained with a constant star formation rate over 0.2-0.5 Myr and an underlying two-step power-law IMF with two free parameters: the slope of the low mass part α_1, and the mass at which the slope changes $M_{\rm flat}$. $dN/d\log M_\star \propto M_\star^{-1.7}$ for the higher mass part, in accordance with recent IMFs. **b)** The mass function for the Class II sources in ρ Ophiuchi. The bold dashed vertical line shows the brown dwarf domain to the left. The completeness limit is at 0.055 $M_\odot$. The best two-step power-law IMF is characterized by the two slopes α_1 and α_2, and the mass where the slope changes, $M_{\rm flat}$. See Bontemps et al. (2001) for more information.

7. Conclusions

The ISO observations have provided a fundamental database for studying the earliest stages of stellar evolution.

From the ISO spectroscopic and photometric observations it has been possible to trace the evolution of the dust and gas emission properties during the earliest stages of stellar formation. The appearence of a new protostar and the gradual dispersal of the initial dusty envelope is evidenced by the change in the shape of the mid and far-IR SEDs of the YSOs. From these SEDs, average dust temperatures are derived, which increase from ∼10 K in the pre-stellar cores, to ∼20–40 K in the Class 0 phase, to temperatures of few hundreds of K in Class I sources, when the appearence of the inner and warmer regions produce significant temperature stratifications in the observed SEDs. For high mass stars, a similar sequence of increasing temperatures can be seen passing from the deeply embedded phase to the UC HII regions.

The ISO spectra, on the other hand, have evidenced for the first time how the prevailing gas excitation mechanisms change during protostellar evolution. In the dense pre-stellar cores the gas is only externally heated by the local interstellar field, while, as soon as a protostellar object is formed, shock excitation, either due to accretion or outflows, dominates the gas heating producing a rich far IR molecular spectrum.

Finally, during the latest accretion phase, the stellar radiation field becomes the dominant source of heating causing, in high mass stars in particular, the excitation of many atomic and ionic forbidden lines.

In addition to the study of individual objects, the ISO photometric surveys have given a census of the IR-excess populations in nearby clouds which is about twice as large as previously known. These complete samples of young YSOs provide a unique database which can be used for the selection of sources to be observed by new ground-based and space-born facilities.

The present and future mid- and far-IR missions, such as Spitzer, Herschel, SOFIA and JWST, will certainly largely improve the observational scenario given by ISO, mainly by providing data acquired with a larger spatial and spectral resolution, and better sensitivity. All of these missions, however, will have in the ISO database a fundamental reference point for the definition and interpretation of their observations.

References

Abergel, A., Bernard, J.P., Boulanger, F., et al., 2002, A&A 389, 239
Alexander, R.D., Casali, M.M., André, P., Persi, P., Eiroa, C., 2003, A&A 401, 613
André P., Ward-Thompson D., Barsony M., 2000, in: Mannings V., Boss A. P., Russell S. S., eds., 'Protostars and Planets IV', University of Arizona Press, p. 59
André P., Ward-Thompson D., Motte F., 1996, A&A, 314, 625
Bacmann A., André P., Puget J.-L., Abergel A., Bontemps S., Ward-Thompson D., 2000, A&A, 361, 555
Beichman C. A., Myers P. C., Emerson J. P., et al. 1986, ApJ, 307, 337
Benson P. J., Myers P. C., 1989, ApJS, 71, 89
Blommaert, J., Siebenmorgen, R., Coulais, A. et al. 2003, 'The ISO Handbook, Volume II: CAM - The ISO Camera', ESA SP–1262
Bontemps, S., André, P., Kaas, A.A., et al., 2001, A&A 372, 173
Boogert, A.C.A., Ehrenfreund, P., Gerakines, P.A., et al. 2000, A&A, 353, 349
Boogert, A.C.A., Hogerheijde, M.R., Ceccarelli, C. et al. 2002, ApJ, 570, 708
Boonman, A.M.S. & van Dishoeck, E.F. 2003, A&A, 403, 1003
Brooks, K.J., Cox, P., Schneider, N., et al., 2003, A&A, 412, 751
Ceccarelli, C., Boogert, A.C.A., Tielend, A.G.G.M., Caux, E., Hogerheijde, M.R., Parise, B., 2002, A.&A., 395, 863
Ceccarelli, C., Castets, A., Caux, E., Loinard, L., Molinari, S., Tielens, A.G.G.M., 2000, A.&A., 355, 1129
Cernicharo, J., Perez-Martinez, S., González-Alfonso, et al. 1999, in The Universe as seen by ISO, ed. P. Cox & M.F. Kessler, ESA-SP 427, p. 651
Cesarsky, C.J. et al. 1996, A&A 315, L32
Clegg, P.E. et al. 1996, A&A 315, L38
Correia, J., Griffin, M., Saraceno, P., 2004, A&A, 418, 607
Churchwell, E. 2002, ARA&A, 40, 27

de Graauw, T. et al. 1996, A&A 315, L49
Foster P. N., Chevalier R. A., 1993, ApJ, 416, 303
Froebrich, D., Smith, M.D., Eislöffel, J., 2002, A.&A., 385, 239
Froebrich, D., Smith, M.D., Hodapp, K.W., Eislöffel, J., 2003, A.&A., 346, 163
Gålfalk, M., 1999, Master Thesis, Stockholm University, see www.astro.su.se/English/thesis/MagnusG_xjobb.pdf
Gålfalk, M., Olofsson, G., Kaas, A.A., et al., 2004, A&A 421, 623
Gerakines, P.A., Whittet, D.C.B., Ehrenfreund, P., et al. 1999, ApJ, 522, 357
Gibb, E.L., Whittet, D.C.B., Boogert, A.C.A., Tielens, A.G.G.M., 2004, ApJSS, 151, 35
Giannini, T., Nisini, B., Lorenzetti, D., 2001, ApJ, 555, 40
Giveon, U., Sternberg, A., Lutz, D., Feuchtgruber, H., & Pauldrach, A.W.A. 2002, ApJ 566, 880
González-Alfonso, E., Cernicharo, J., van Dishoeck, E.F., Wright, C.M. & Heras, A. 1998, ApJ, 502, L169
Greene, T.P., Wilking, B.A., André, P., Young, E.T., Lada, C.J., 1994, ApJ 434, 614
Gry, C., Swinyard, B., Harwood, A. et al. 2003, 'The ISO Handbook, Volume III: LWS - The Long Wavelength Spectrometer', ESA SP–1262
Harwit, M., Neufeld, D.A., Melnick, G.J., Kaufman, M.J. 1998, ApJ, 497, L105
Hollenbach D., 1997, in Herbig-Haro flows and the birth of low mass stars. IAU symposium no. 182, Reipurth B., Bertout C. (eds.), p.181
Hollenbach D., Tielens, A.G.G.M., 1997, ARA&A, 35, 179
Kaas, A.A., Olofsson, G., Bontemps, S., et al., 2004, A&A, 421, 623
Kaas, A.A., Olofsson, G., Bontemps, S., et al., 1999, In: The Universe as seen by ISO, ESA SP-427, p. 493
Kaas, A.A., Bontemps, S., 2000, In: From Darkness to Light: Origin and Evolution of Young Stellar Clusters, eds. Montmerle, T, André, P., ASP Conf. Proc. 243, p. 367
Kaufman, M.J., Neufeld, D.A., 1996, ApJ, 456, 611
Keane, J.V., Tielens, A.G.G.M., Boogert, A.C.A., Schutte, W.A., & Whittet, D.C.B. 2001, A&A, 376, 254
Kessler, M.F. et al. 1996, A&A 315, L27
Kessler, M.F., Mller, T.G., Leech, K. et al. 2003, 'The ISO Handbook, Volume I: ISO - Mission & Satellite Overview', ESA SP–1262
Kirk J. M., Ward-Thompson D., André P., 2004, MNRAS, in press
Krause, O., Lemke, D., Tóth, L.V., Klaas, U., Haas, M., Stickel, M. & Vavrek, R. 2003, A&A, 398, 1007
Kurtz, S., Cesaroni, R., Churchwell, E., Hofner, P. & Walmsley, C.M. 2000, in Protostars & Planets IV, ed. V. Mannings et al. (Tucson: University of Arizona), p. 299
Lada., C., 1999, in The Origin of Stars and Planetary Systems, ed. C.J Lada and N.D. Kylafis (Kluwer, Dordrecht)
Lada, C.J., Wilking, B.A., 1984, ApJ 287, 610
Lahuis, F. & van Dishoeck, E.F. 2000, A&A, 355, 699
Larsson, B., Liseau, R., Men'shchikov, A.B., et al. 2000, A.&A., 363, 253
Larsson, B., Liseau, R., Men'shchikov, A.B., 2002, A.&A., 386, 1055
Laureijs, R.J., Klaas, U., Richards, P.J. et al. 2003, 'The ISO Handbook, Volume IV: PHT - The Imaging Photo-Polarimeter', ESA SP–1262
Leech, K., Kester, D., Shipman, R. et al. 2003 ESA SP–1262

Lefloch, B., Cernicharo, J., Cabrit, S., Noriega-Crespo, A., Moro-Martín, A., Cesarsky, D., 2003, ApJ, 390, L41
Lehtinen, K., Haikala, L.K., Mattila, K., Lemke, D., 2001, A&A, 367, 311
Lemke, D. et al. 1996, A&A 315, L64
Liseau, R., Giannini, T., Nisini, B., et al. 1997,in Herbig-Haro Flows and the Birth of Low Mass Stars, ed. B. Reipurth & C. Bertout, 111
Liseau, R., Ceccarelli, C., Larsson, B. et al., 1996, A.&A., 315, L181
Maret, S., Ceccarelli, C., Caux, E., Tielens, A.G.G.M., Castets, A., 2002, A.&A., 395, 573
Molinari, S., Noriega-Crespo, A., Ceccarelli, C., et al. 2000, ApJ, 538, 698
Molinari, S., Noriega-Crespo, A., Spinoglio, L., 2001, ApJ, 547, 292
Moro-Martín, A., Noriega-Crespo, A., Molinari, S., Testi, L., Cernicharo, J., Sargent, A., 2001, ApJ, 155, 146
Motte, F., André, P., Neri, R., 1998, A&A 336, 150
Motte F., André P., Ward-Thompson D., Bontemps S., 2001, A&A, 372, L41
Myers P. C., Benson P. J., 1983, ApJ, 266, 309
Myers P. C., Heyer M., Snell R. L., Goldsmith P. F., 1988, ApJ, 324, 907
Neufeld, D.A., Melnick, G.J., Harwit, M., 1998, ApJ, 506, L75
Nisini, B., 2003, in: Proc. of the Symposium 'Exploiting the ISO Data Archive - Infrared Astronomy in the Internet Age', C. Gry, S.B. Peschke, J. Matagne et al. eds., ESA SP-511, p. 111
Nisini, B., Benedettini, M., Giannini, T., et al., 1999, A.&A., 350, 529
Nisini, B., Benedettini, M., Giannini, T., Codella, C., Lorenzetti, D., Di Giorgio, A., Richer, J.S. 2000, A.&A., 360, 297
Nisini, B., Giannini, T., Lorenzetti, D., 2002, ApJ, 574, 246
Nordh, L., Olofsson, G., Abergel, A., et al., 1996, A&A 315, L185
Olofsson, G., Huldtgren, M., Kaas, A.A., et al., 1999, A&A 350, 883
Peeters, E., Martín-Hernández, N.L., Dufour, F., et al. 2002, A&A, 381, 571
Persi, P., Marenzi, A.R., Olofsson, G., et al., 2000, A&A 357, 219
Persi, P., Marenzi, A.R., Gómez, M., Olofsson, G., 2003, A&A 399, 995
Reipurth, B., Bally, J., 2001, ARA&A, 39, 403
Rosenthal, D., Bertoldi, F. & Drapatz, S. 2000, A&A 356, 705
Saraceno P., Nisini B., Benedettini M., et al., 1999, Proc. of the Conference 'The Universe as seen by ISO',P. Cox & M. Kessler eds., ESA SP-427, p. 575
Shu F. H., 1977, ApJ, 214, 488
Smith, M.D., Froebrich, D., Eislöffel, J., 2003, ApJ, 592, 245
van den Ancker, M.E., Tielens, A.G.G.M. & Wesselius, P.R. 2000, A&A, 358, 1035
van der Tak, F.F.S., van Dishoeck, E.F., Evans, N.J. & Blake, G.A. 2000, ApJ, 537, 283
van Dishoeck, E.F. 2004, ARA&A, 42,119
van Dishoeck, E.F., Wright, C.M., Cernicharo, J., González-Alfonso, E., de Graauw, Th., Helmich, F.P., Vandenbussche, B. 1998, ApJ, 502, L173
Ward-Thompson D., André P., Kirk J. M., 2002, MNRAS, 329, 257
Ward-Thompson D., Motte F., André P., 1999, MNRAS, 305, 143
Ward-Thompson D., Scott P. F., Hills R. E., André P., 1994, MNRAS, 268, 276
White, G.J., Liseau, R., Men'shchikov, A.B., et al., 2000, A.&A., 364, 741
Whitworth A. P., Bhattal A. S., Francis N., Watkins S. J., 1996, MNRAS, 283, 1061
Whitworth A., Summers D., 1985, MNRAS, 214, 1
Wilgenbus D., Cabrit S., Pineau Des Forêts, Flower D., 2001, "From Darkness to Light: Origin and Evolution of Young Stellar Clusters", ASP Conference Proceedings, Vol. 243, p.347

Williams J. P., Blitz L., McKee, C. F., 2000, in: Mannings V., Boss A. P., Russell S. S., eds., 'Protostars and Planets IV', University of Arizona Press, p. 97
Wright, C.M., Drapatz, S., Timmermann, R., et al., 1996, 315, L301
Wright, C.M., van Dishoeck, E.F., Black, J.H., Feuchtgruber, H., Cernicharo, J., González-Alfonso, E. & de Graauw, Th. 2000, A&A, 358, 689